Review article **Open Access**

Martijn J.R. Heck*

Highly integrated optical phased arrays: photonic integrated circuits for optical beam shaping and beam steering

DOI 10.1515/nanoph-2015-0152
Received December 10, 2015; revised February 2, 2016; accepted February 7, 2016

Abstract: Technologies for efficient generation and fast scanning of narrow free-space laser beams find major applications in three-dimensional (3D) imaging and mapping, like Lidar for remote sensing and navigation, and secure free-space optical communications. The ultimate goal for such a system is to reduce its size, weight, and power consumption, so that it can be mounted on, e.g. drones and autonomous cars. Moreover, beam scanning should ideally be done at video frame rates, something that is beyond the capabilities of current opto-mechanical systems. Photonic integrated circuit (PIC) technology holds the promise of achieving low-cost, compact, robust and energy-efficient complex optical systems. PICs integrate, for example, lasers, modulators, detectors, and filters on a single piece of semiconductor, typically silicon or indium phosphide, much like electronic integrated circuits. This technology is maturing fast, driven by high-bandwidth communications applications, and mature fabrication facilities. State-of-the-art commercial PICs integrate hundreds of elements, and the integration of thousands of elements has been shown in the laboratory. Over the last few years, there has been a considerable research effort to integrate beam steering systems on a PIC, and various beam steering demonstrators based on optical phased arrays have been realized. Arrays of up to thousands of coherent emitters, including their phase and amplitude control, have been integrated, and various applications have been explored. In this review paper, I will present an overview of the state of the art of this technology and its opportunities, illustrated by recent breakthroughs.

Keywords: silicon photonics; lidar; free-space optical communications; III/V photonics; photonic integrated circuits.

1 Introduction

Optical beam shaping is the generation of a narrow, low-divergence, beam of laser light in the visible or infrared wavelength range. Optical beam steering is the dynamic pointing or scanning of such beams, preferably over a wide angle. Narrow, steerable beams of laser light find ubiquitous applications in many different fields. One main application is free-space optical communication, where the laser beam is modulated to transmit data, typically up to the gigabit-per-second range, over distances of multiple kilometers. Beam steering is required to compensate the relative displacement of transmitter and receiver. An advantage over wireless radio networks is that the laser beam between sender and receiver can be narrow, so there is a low probability of interception and, hence, of eavesdropping, which makes the link secure.

Another main application is 3D imaging and mapping, such as Lidar systems. In this application, the laser beam is scanned and the distance to a point is measured using reflection or scattering, thereby creating a 3D image of the environment. Already, Lidar systems find ubiquitous applications in remote sensing, but emerging technologies like autonomous car and drone navigation will dramatically increase the use of such systems in the near future.

And many more applications can be found. In the field of imaging, projectors and heads-up display screens are enabled by fast-scanning light beams. For electronic warfare, the laser beam can be used to precision guide missiles to their target. Alternatively, the laser beam can

***Corresponding author: Martijn J.R. Heck,** Department of Engineering, Aarhus University, Finlandsgade 22, 8200 Aarhus, Denmark, e-mail: mheck@eng.au.dk

©2016, Martijn J.R. Heck, published by De Gruyter.
This work is licensed under the Creative Commons Attribution-NonCommercial-NoDerivatives 3.0 License.

be used for countermeasures, e.g. by interfering with or blinding the optical sensors of such precision-guided missiles. For lithography, laser writing and additive manufacturing, e.g. 3D printing, the fast-scanning laser beams define the patterns and shapes.

Systems that can generate, shape, and steer a narrow optical beam tend to be rather bulky, as they often consist of mechanical assemblies, based on opto-mechanical systems. Such systems are expensive, relatively slow, and sensitive to temperature changes and mechanical shocks, which limit their use typically to static, ground-based deployment. Efforts to further miniaturize such systems include the use of micro-electromechanical mirrors (MEMS) and liquid-crystal-based spatial light modulators. Nowadays, compact optical projectors are realized using these technologies, for example, based on light-emitting diodes (LEDs) combined with digital light processing (DLP) or liquid-crystal on silicon (LCOS) chips. However, scanning and tuning speed for these technologies are limited to the millisecond range, which limits their use. For example, a Lidar system for real-time, frame-rate imaging would require tuning in the microsecond to nanosecond range.

The ultimate goal for a beam steering system is to reduce its size, weight, and power consumption (SWaP), so that it can be mounted on small vehicles, e.g. drones, cars, and satellites, or can be carried as a handheld device, and, for example, be part of future smartphones. In this paper, I will review the state of the art in the use of photonic integrated circuits (PICs) for beam generation, shaping, and steering based on optical phased array (OPA) technology. Relevant metrics, including beam width and steering angle, will be discussed, as well as potential power scaling. It will be shown that PICs can generate narrow beams, have a wide steering angle, and can have tuning speeds in the megahertz to gigahertz range. Moreover, their compact footprint allows for miniaturization of the full system. Such PICs operate in the infrared wavelength range, which is preferred for, e.g. communication and Lidar applications, as such wavelengths are eye-safe.

In this paper, I will first introduce the PIC technology and its advantages for beam shaping and steering in Section 2. Then the principles of OPAs will be introduced in Section 3. In Section 4, the recent achievements in two-dimensional (2D) arrays for beam steering will be discussed. One-dimensional arrays that use wavelength tuning for full 2D steering will be discussed as a relevant alternative implementation in Section 5. In Section 6, I will present an outlook for further research potential and real-world implementation. The conclusions are then summarized in Section 7.

2 Optical phased arrays

Beam shaping can be achieved using OPAs [1, 2]. These are arrays of coherent optical emitters, much like the well-known concept of phased array antennas in radio wave and microwave technology. By controlling the phase and/or amplitude of these emitters, the electro-magnetic field close to the emitters, i.e. the near field, can be fully controlled. This is shown schematically in Figure 1A. To achieve coherent emitters, these have to be fed by a single laser source, as shown, or by an array of phase locked or injection locked lasers.

Sufficiently far away from the emitters, the so-called far field is described by Fraunhofer diffraction theory and is basically the complex Fourier transform of the near field [3]. This relatively straightforward relation makes the design criteria very insightful. Figure 1B–D shows some of the trade-offs that need to be considered. To achieve a narrow beam in the far field, a flat phase profile in the near field is required. The width of the array then determines the width of the far-field beam, scaling inversely. The slope of the near-field phase profile determines the output angle of the beam. This means that by phase tuning the emitters, beam steering is achieved.

A complicating factor is that the emitter array consists of a discrete set of elements, which will lead to typically unwanted side lobes when the emitter spacing is larger than $\lambda/2$, with λ as the wavelength of the optical field in

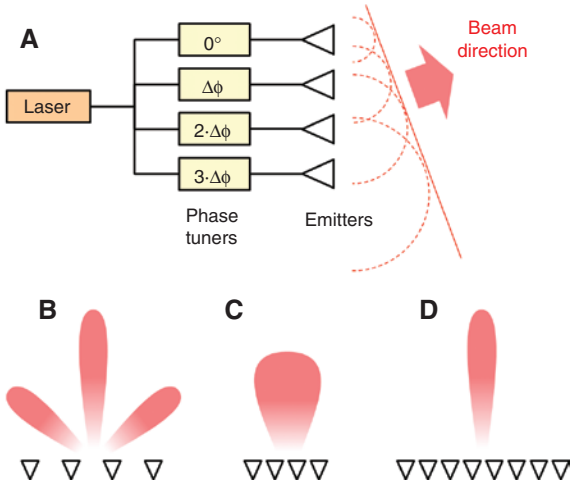

Figure 1: Operation principle of phased arrays.
(A) Schematic of phased array operation, showing a laser feeding an array of emitters. The phase of the output of each emitter can be tuned (yellow boxes) and is shown (dashed red circles). In the far field, these add up to a beam. The design trade-offs are shown for (B) widely spaced emitters (triangles), (C) densely spaced emitters, and (D) increasing the number of emitters. The output beam angle and amplitude are shown schematically in red in (B–D).

the medium of propagation. Such side lobes decrease efficiency and are generally detrimental for applications in Lidar, as they add noise or false positives and, in secure communications, as the link can now be eavesdropped. In the following, we will see that PIC-based emitters typically have a spacing that exceeds this value, which will have to be addressed in the design. This leads to a general trade-off for the number of elements in terms of beam quality versus PIC complexity and for element spacing in terms of field of view, i.e. angle of maximum beam steering and beam width.

3 Photonic integration technology and its advantages for beam steering

PICs combine different photonic functionalities, such as lasers, optical amplifiers, modulators, photodetectors, filters, and/or waveguides, on a single substrate. This combination can be achieved monolithically or heterogeneously, i.e. by using a single material system or by a combination of materials, respectively. PIC technology, as defined in this work, is essentially different from the broader field of "photonic integration" or "integrated optics", as these latter fields also include single components or functionalities realized using various micro-photonic and nano-photonic cleanroom fabrication technologies but without necessarily a clear path and rationale for further integration.

An essential aspect of PIC technology is the necessity for trade-offs. Concessions have to be made to converge to a fabrication process flow that allows for the integration of all required components. This inherently implies that not all components that will compose the PIC will be best in class. Driven by applications in high-bandwidth telecom and datacom applications, PIC technology seems to converge on only a limited set of platforms for large-scale integration of hundreds to thousands of components per PIC. These are silicon photonic [4, 5], indium phosphide [6], and silica or silicon nitride platforms [7]. Combinations of these technologies can be realistically considered, too, e.g. heterogeneous silicon indium phosphide integration, also known as the hybrid silicon platform [8]; the integration of silicon with silicon nitride [9, 10]; or even silicon, silicon nitride, and indium phosphide all together in a single process flow [11, 12]. For illustrative purposes, an example of a typical silicon photonic technology is shown in Figure 2.

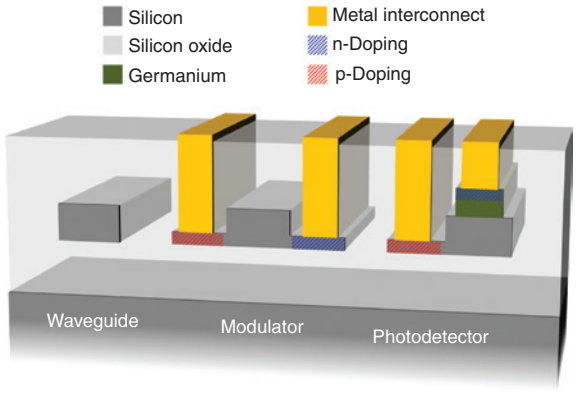

Figure 2: Schematic of components in silicon photonics technology. The components can be fabricated on a silicon substrate, using CMOS-compatible processes and processing infrastructure. The silicon waveguide confines and guides light. Electrical contacts on the modulator waveguide allow for carrier injection or depletion, thereby changing the refractive index of the waveguide and creating a phase or amplitude modulator. The photodetector waveguide has a germanium layer, which absorbs the light. Carriers are generated upon absorption, which are detected as an electrical current.

PIC technology is well suited for the integration of massive amounts of parallel components, as required for optical phased arrays. Micro and nanofabrication techniques commonly used in the electronics industry are used to make the platforms robust, reproducible, and of high quality. On the other hand, parallel integration avoids the issues that would arise with the lack of feasible optical isolators in PIC technology. Figure 3 shows the exponential growth of complexity of PIC technology, illustrating its potential for massive parallel integration.

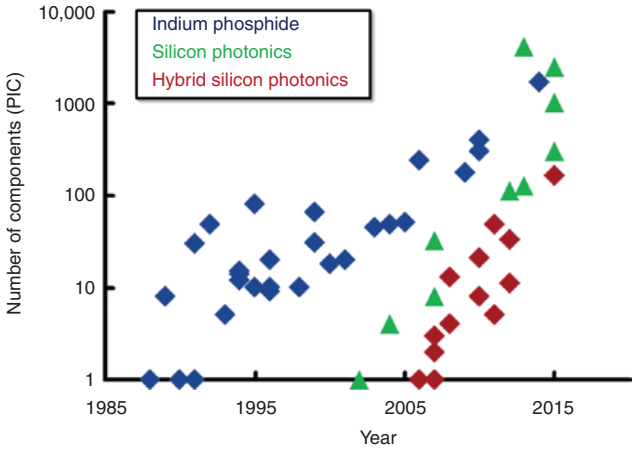

Figure 3: Evolution of the number of components on PICs over the last 30 years. Indium phosphide (blue), silicon photonic (green), and hybrid silicon (red) PICs are included. Figure was based on the data from Ref. [8] and expanded with some recent results.

State of the art in indium phosphide, silicon photonics, and hybrid silicon photonics is shown in this figure, and I will discuss examples of all these technologies for OPAs in this paper.

A key advantage of PICs is that control is electro-optical, which means that there is no mechanical motion and bandwidth can be very high, well into the gigahertz range. Moreover, lithographic accuracy of the fabrication process ensures optical path length control well into the sub-wavelength regime, which is essential for avoiding phase errors. This means that PICs are in principle ideal candidates for low SWaP and robust OPAs. In the following, I will show the current state of the art in using PICs for OPAs.

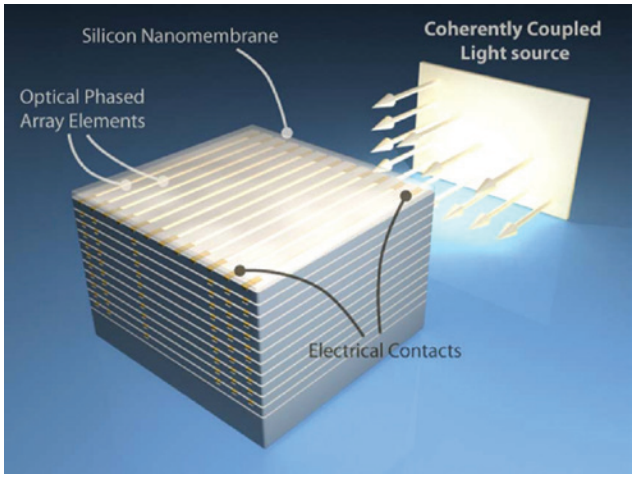

Figure 4: Envisioned stacking of 1D edge-emitting silicon photonic OPAs to realize a 2D emitter array, injection locked by a single master laser for coherent OPA emission. Reprinted with permission from Ref. [15]. Copyright 2010, American Vacuum Society.

4 Optical phased arrays with individually tunable emitters

Conceptually, the most straightforward approach to integrate beam shaping and steering in two dimensions is to make use of a 2D array of coherent emitters so that each can be controlled in terms of output phase and, possibly, power. Following from the design criteria, as discussed above, such arrays should be as large as possible, with the emitters closely spaced. Initial work in this field first focused on one-dimensional (1D) arrays fabricated in indium phosphide [13] and silicon photonic technology [14]. For example, this latter realization used a 12-channel edge emitting array, tunable over 32°. Even though thermo-optic phase tuning was used, its 100-kHz bandwidth still outperformed liquid-crystal technology by two orders of magnitude. A non-uniform spacing was used to suppress unwanted side lobes. Using rod lenses, such 1D arrays can be used to achieve 1D beam steering while still keeping the beam narrow in both dimensions. To achieve 2D beam steering, a stack of 1D silicon photonic PICs was suggested in Ref. [15]. This approach is shown schematically in Figure 4. Subarrays with varying emitter spacing in both transverse directions can be used to suppress side lobes. Another possible approach to expand the 1D array of emitters, inherent to planar edge-emitting PICs, into a 2D array is to use a so-called photonic lantern [16].

A more elegant approach is to realize the full 2D emitter array on the PIC plane or surface. Especially high-contrast silicon photonics is well suited for this, making use of vertical grating couplers [17, 18]. A 64×64 array consisting of a total of 4096 emitters was developed by Sun et al. and is shown in Figure 5 [19]. The emitter pitch is 9 µm, i.e. well beyond half the used wavelength of 1.55 µm, so multiple far-field images are formed. This short grating length allows for an optical bandwidth of hundreds of nanometers. In this implementation, the phase is encoded lithographically by tuning the waveguide lengths, which leads to a relative delay. The output field is, hence, static.

Active beam shaping and steering was achieved in the same work, by adding thermo-optic phase tuners to the arms. This allows for arbitrary phase shaping of the field above the emitters. However, uniform emission of the emitters leads to a non-Gaussian beam in the far field. More specifically, a beam shape corresponding to a sinc function will result if a square aperture is considered. This was also experimentally observed, as shown in Figure 6. By apodizing the near field of an 8×8 array of emitters and using a similar silicon photonic OPA technology as that of Ref. [19], a clean Gaussian far-field beam shape was achieved, as also shown in Figure 6 [20]. The static, lithographically designed, amplitude control and the tunable phase control enable the generation of arbitrary optical beam profiles.

The work by Abediasl et al. took this approach a few steps further and presented a silicon photonic PIC that includes both active amplitude and phase control of an 8×8 array, using thermo-optic tuning, for full arbitrary dynamic beam shaping [21]. This work also addresses the issue that in real-world systems, the PIC needs to be accompanied by electronic drivers. Although one can envision, e.g. flip-chip bonded driver circuits for such massively integrated PICs, an elegant approach is to integrate electronics and photonics on a single circuit, using a single process. This work achieved this using a commercial IBM 7RF-SOI CMOS

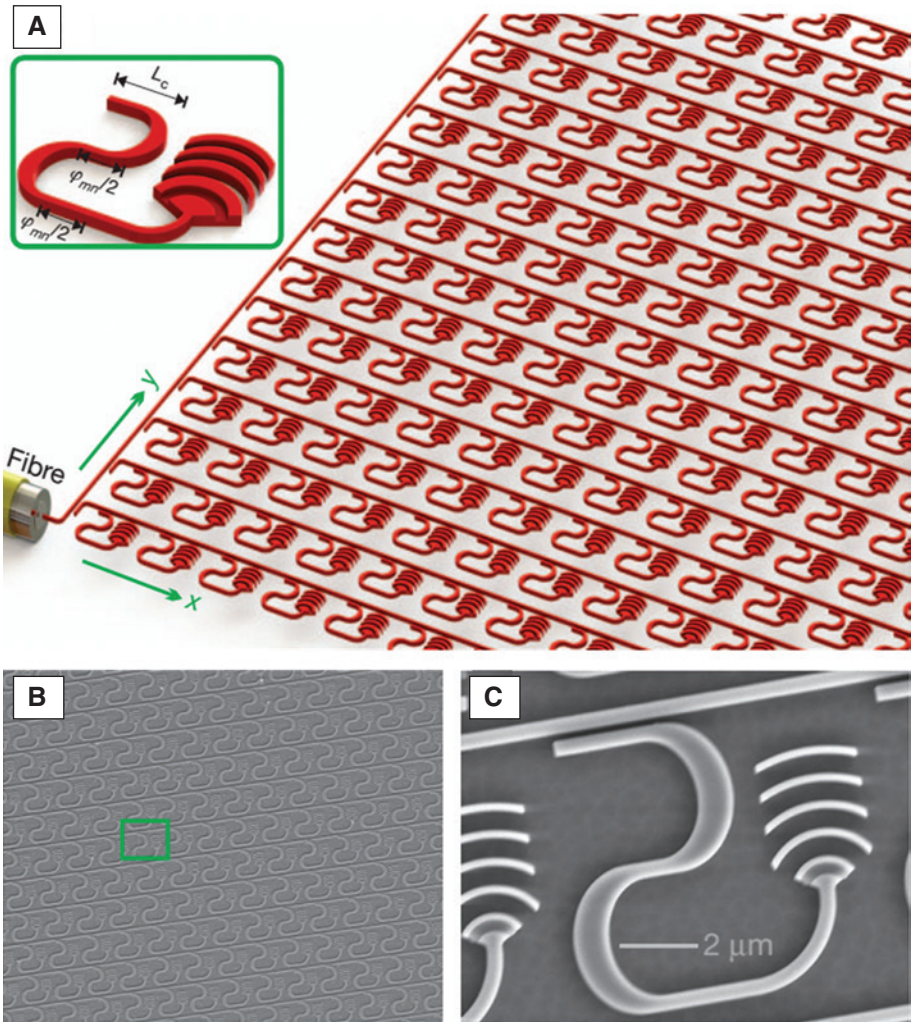

Figure 5: Silicon photonic two-dimensional optical phased array.
(A) Schematic illustration of a two-dimensional emitter array. Laser light is coupled into the input waveguide on the chip and distributed equally over the array. Grating couplers act as emitters by coupling the laser light out of plane. A scanning-electron microscope picture of the array is shown in (B) and a close-up of the grating emitter is shown in (C). Reprinted by permission from Macmillan Publishers Ltd. Nature [19], copyright 2013.

process, for an overall integration density of 300 optical and 74,000 electrical components, as shown in Figure 7. The phase tuner current is controlled by 7-bit digital-to-analog converters. This chip can be used both as a receiver and as a transmitter for free-space communications.

Some interesting applications of these 2D silicon photonic OPAs have been identified and explored. In Ref. [22], a 4×4 array was realized using diode-based phase tuners, making use of carrier injection. In comparison to the thermo-optic effect, this electro-optic effect is very fast, leading to tuning bandwidths of 200 MHz. Such fast beam steering can be used to project an image by vector or raster scan. A picture of the PIC and the projected image is shown in Figure 8. Such a PIC enables low-cost 3D imaging and holography, without lenses and without mechanical movement.

The application as a coherent imager was explored in Ref. [23]. A 4×4 array was used to emit a beam that was modulated according to a time-domain frequency modulated continuous wave (FMCW) ranging scheme, similar to FMCW radar systems. This PIC integrates the optical signal processing and detection. A depth resolution of 15 µm and a lateral resolution of 50 µm, at a range up to 0.5 m were achieved using this 3D imaging approach.

Although some of the presented PICs allow for both phase and amplitude control of the emitters, it has to be noted that this is not always an attractive option. Amplitude control by attenuating the light effectively decreases the wall-plug efficiency of the OPA, in terms of optical output power versus electrical input power. However, with algorithms typically used in holography, e.g. the

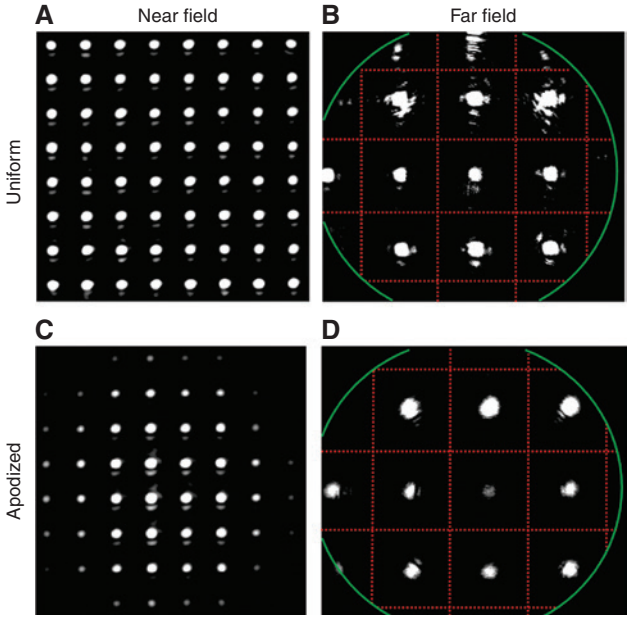

Figure 6: Apodization to suppress side-lobes.
Measured (A, C) near-field emission and (B, D) far-field optical beam profile, obtained using a uniform and Gaussian-apodized 8×8 OPA, respectively. Reprinted by permission of The Optical Society [20].

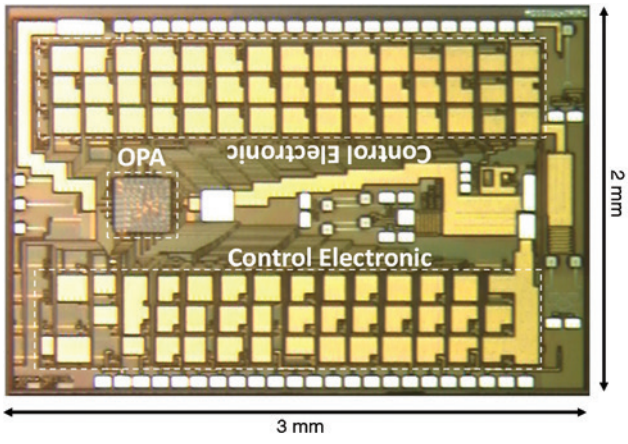

Figure 7: Microscope picture of an 8×8 OPA, monolithically integrated with control electronics in a 180-nm CMOS process. Reprinted by permission of The Optical Society [21].

Gerchberg-Saxton algorithm [24, 25], phase-only beam shaping can be used to obtain arbitrary far-field images.

The OPAs reviewed in this section make use of external laser sources, coupled to the PIC, to generate the light. This is necessary, as most realizations are based on silicon photonic PICs, for which no efficient integrated light sources are available. Mature packaging approaches are available, though, to attach the laser to a silicon photonic chips, e.g. as discussed in Ref. [17]. In the next section, I will review PICs that also include on-chip laser sources.

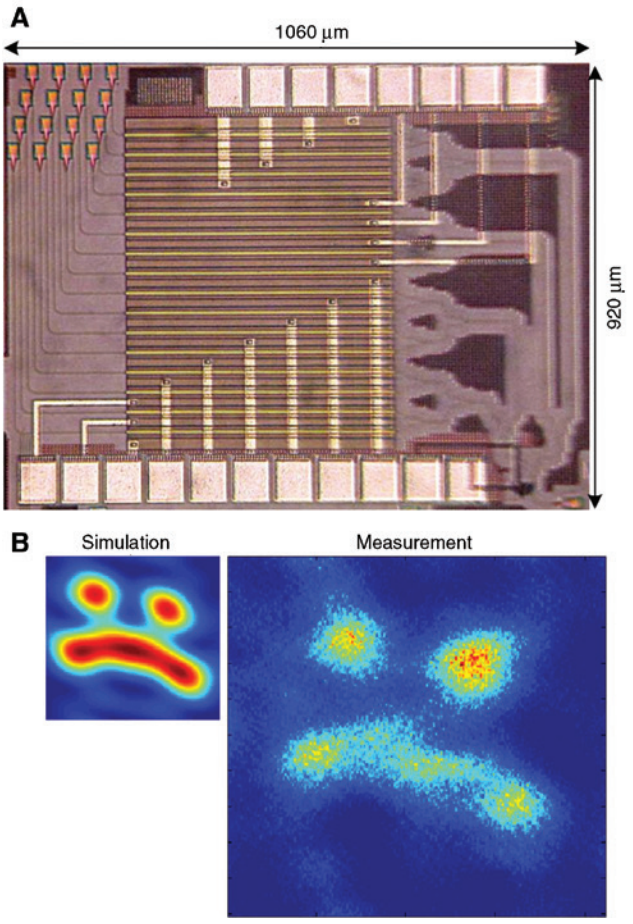

Figure 8: Projection chip based on silicon photonics.
(A) Microscope picture of a 4×4 integrated OPA, realized on silicon, with high-speed phase control per channel. (B) Projected image of a "smiley" obtained by using a fast vector scan of the beam spot, showing simulated (left) and experimental (right) results. Reprinted by permission of The Optical Society [22].

5 Optical phased arrays using tunable lasers for beam steering

As is clear from the above, decreasing the beam width requires an increased number of emitters in the OPA. For a fixed spacing, the beam width scales inversely with the number of emitters N in a linear array, as was shown in Figure 1. This means that for a square 2D array, consisting of $N \times N$ emitters, the beam width scales inversely with N^2. As every emitter needs to be phase- and, possibly, amplitude-controlled, this scaling implies that the control electronics quickly become the bottleneck and possibly prohibitive. This is especially the case when large currents and fast tuning in the tens of megahertz range are required for the hundreds or even thousands of emitters.

An alternative approach makes use of the dispersive nature of the surface emitting gratings that are used in

many of the OPA examples discussed in Section 4 and that are discussed in detail in, e.g. Refs. [17, 18]. The direction of light emission in a grating emitter is dependent on the wavelength of light, which gives an additional parameter to achieve beam steering. Wavelength-tunable lasers are common in telecommunications and have been developed typically in indium phosphide technology for commercial purposes [26] but have been realized as proof-of-principle demonstrations in the silicon photonic platform by hybrid [27] and heterogeneous integration [28, 29].

An interesting aspect of these vertical grating couplers, which are second-order gratings, is that the grating period is below half a wavelength in free-space. This means that only a single diffraction order is emitted, and no side lobes appear along the grating direction. A disadvantage is that the phase relation in a grating is fixed and linear for uniform gratings. However, when narrow beam shaping and steering is the goal, this approach works well. Beam width can be simply controlled by the length of the grating, with longer gratings leading to more narrow beams. By creating an array of such grating emitters, that are phase-controlled and have coherent output, beam shaping and steering in the perpendicular direction is achieved, as discussed in Section 4. This is shown schematically in Figure 9. Unlike the N^2-scaling of beam width with two-dimensional array size, for this approach, the beam width only scales with N, as the other dimension can be addressed by changing grating length. This severely decreases control electronics complexity by one to two orders of magnitude for the designs discussed here. In the following, I will discuss some examples.

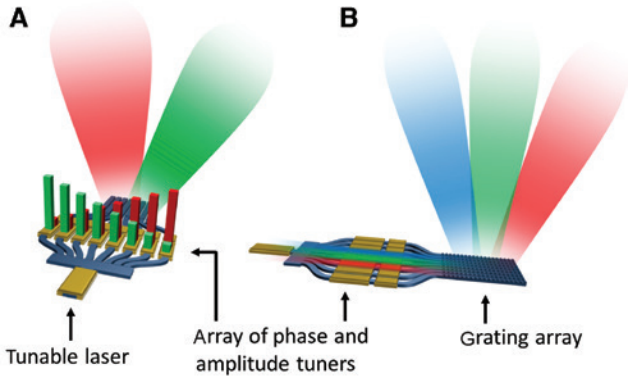

Figure 9: Operation principle of OPAs using wavelength steering. (A) By applying and changing a linear phase profile over the phase tuners, the beam is formed and steered in a direction perpendicular to the grating emitters. Red and green bars schematically indicate the amount of phase tuning. (B) In the direction of the grating emitter, the beam is steered by changing the wavelength of the light, using a tunable laser. Three different wavelengths are schematically shown in red, green, and blue.

A first realization was reported in Ref. [30], implementing an array of 16 parallel grating couplers on the silicon photonic platform. An off-chip tunable laser was used, operating around 1.55 μm. Thermo-optic heating, using a single contact only, was used for 2.3° transverse steering. By wavelength tuning, 14.1° steering was achieved in the longitudinal direction. An improved version, with 16 separately tunable channels and gratings, was presented in Ref. [31]. Two-dimensional beam steering was achieved with a total field of view of 20° by 14° and with a beam width of 0.6° by 1.6°. A hill-climber algorithm was used to optimize the phase tuning settings, and background peak suppression of over 10 dB was achieved over the full window. Examples of beam shaping and tuning are shown in Figure 10. Alternative implementations include a 4×4 short grating array that was used for steering in one dimension only [32] and an OPA that can be steered in two dimensions using wavelength tuning only [33]. This latter realization is shown in Figure 11 and was achieved by implementing different waveguide lengths before the gratings, which leads to a cyclic tilt in the transverse phase front when wavelength is varied. Steering ranges of 15° in the longitudinal direction and 50° in the transverse direction were measured for a wavelength shift of 100 nm. To increase accuracy of etch depth, and hence reproducibility of grating coupling strength, and to increase grating top emission, a polycrystalline silicon overlay was used for the OPA in Ref. [34], based on the grating coupler concepts laid out in Ref. [35], indicating that emission efficiencies of -1.6 dB should be feasible.

All the above-mentioned realizations used an off-chip tunable laser source. Using hybrid silicon technology or indium phosphide technology, the laser source can be integrated on the same PIC. This was first shown in Ref. [36], where a single-wavelength laser was integrated with eight grating couplers for 1D beam steering across a 12° field of view in the transverse direction. Full 2D beam steering was achieved with a 32-channel hybrid silicon PIC that includes a tunable laser among an overall of 164 integrated components [37]. PIC schematic and realization are shown in Figure 12. Beam steering over 23° by 3.6° was achieved, with a beam width of 1° by 0.6°. A similar approach was used to realize an indium phosphide PIC for monolithically integrated beam generation, shaping, and steering [38]. This layout is shown in Figure 13. This PIC shows the advantage of high-quality optical amplifiers and tunable lasers. Realizing an efficient and reproducible grating coupler is more challenging in the indium phosphide technology, however. The bandwidth of indium phosphide modulators, which are typically based on field effects like the Pockels effect, is larger than the bandwidth of silicon

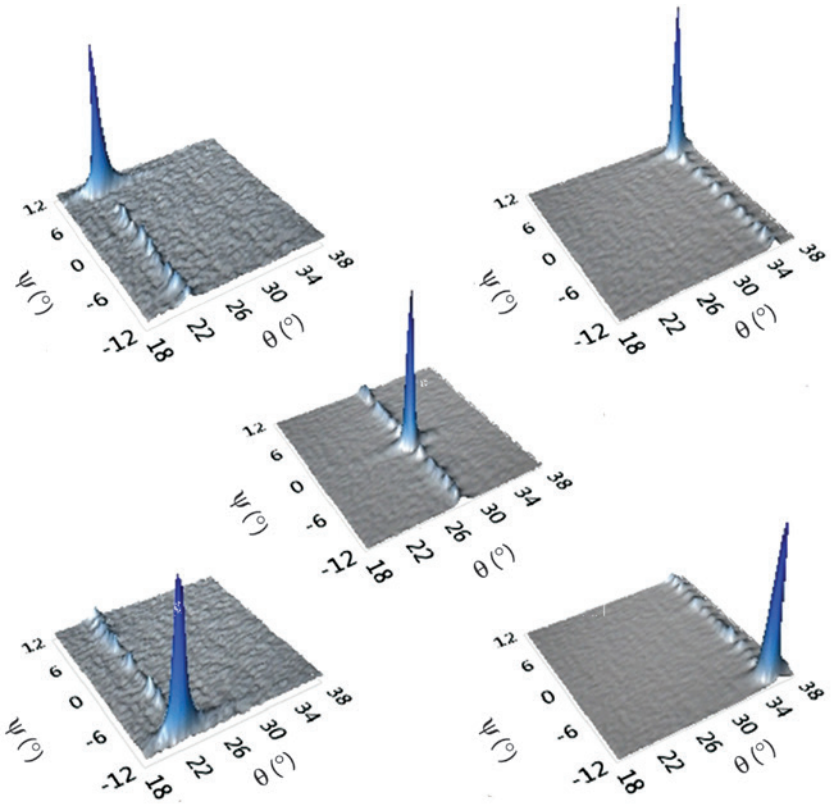

Figure 10: Plots of the beam profiles obtained with the silicon photonic OPA presented in Ref. [31], showing steering over the field of view, which is defined to exclude secondary peaks. Reprinted (adjusted) by permission of The Optical Society.

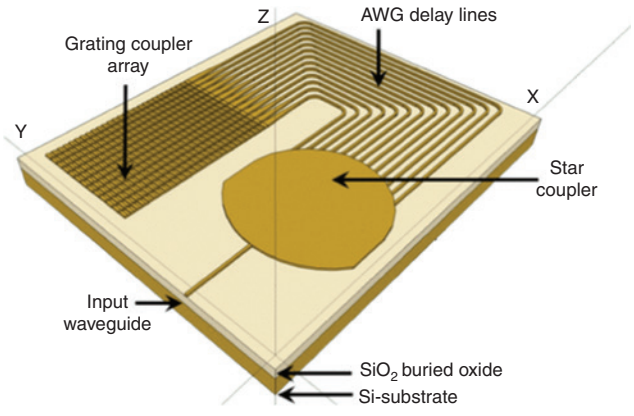

Figure 11: Schematic of a 2D beam scanner realized in a silicon photonic PIC and tunable in two dimensions by tuning the wavelength of the light at the input waveguide only [33].

modulators, which are based on carrier effects, which means that the tuning speed of indium phosphide based OPAs can more easily scale into the gigahertz regime.

The far-field beam shape should be optimized by grating, i.e. near field, apodization, as was shown in Figure 6. In the transverse direction, this can be achieved using variable coupling. An elegant approach is to use a star coupler, as shown in Figure 11. As the light from the input waveguide diffracts with a more or less Gaussian profile inside the slab, the power is distributed over the array of gratings with the same Gaussian distribution. This leads to a clean, Gaussian far field in the transverse direction. In the longitudinal direction, the field needs to be apodized along the grating emitter. This can be achieved by tailoring the grating strength along the waveguide, typically starting low and ending high. One theoretical way to achieve this is to increase grating groove etch depth along the grating, but this is practically unfeasible. In a realistic implementation, one needs to conform to the process flow for PIC fabrication. Work presented in Ref. [39, 40] for silicon photonic gratings shows that by simultaneously varying the grating period and duty cycle, the grating strength can be tuned while keeping the emission angle constant. This avoids varying etch depth and keeps the design fully compatible with the mature fabrication processes [4, 5].

Although no practical applications have been shown in literature using these wavelength-steerable OPAs, one

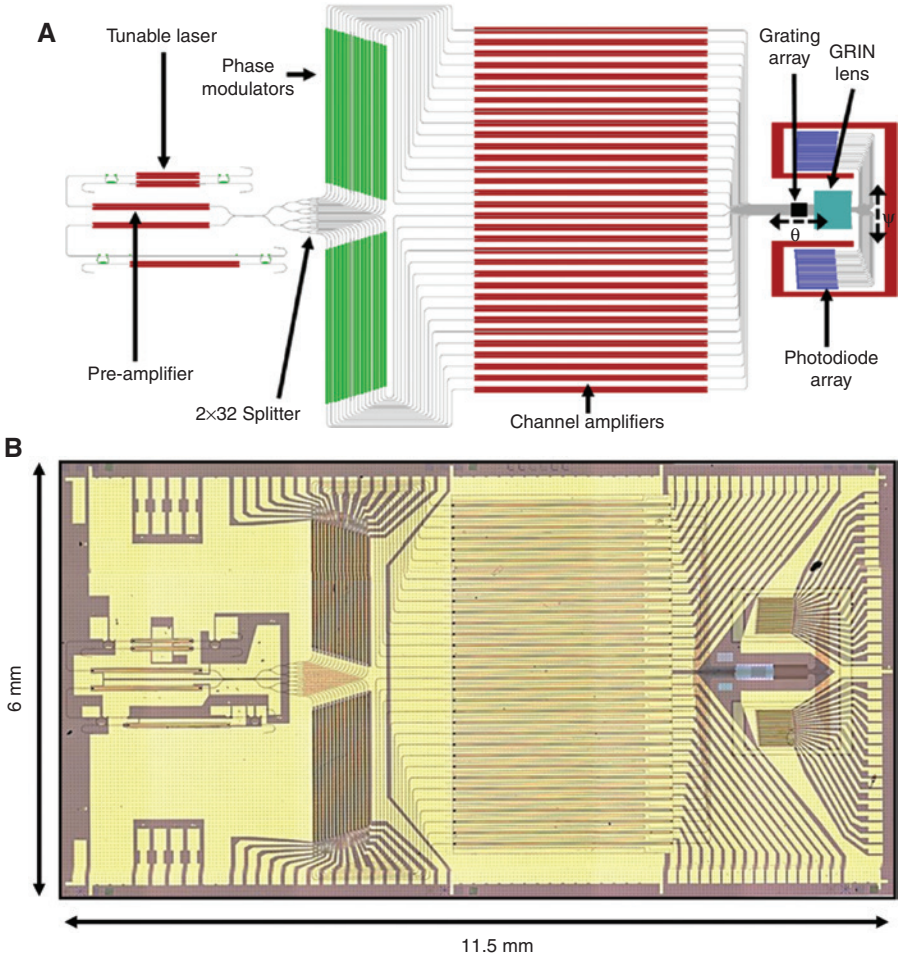

Figure 12: (A) Mask layout of a fully integrated hybrid silicon OPA, including tunable laser sources, optical pre-amplifiers (SOA), phase tuning and grating emitters in 32 channels. A GRIN lens images the remaining beam power into a photodetector array, mimicking the far field. (B) Microscope picture of the fully integrated beam-steering hybrid silicon PIC. A total of 164 photonic components were integrated. Reprinted by permission of The Optical Society [37].

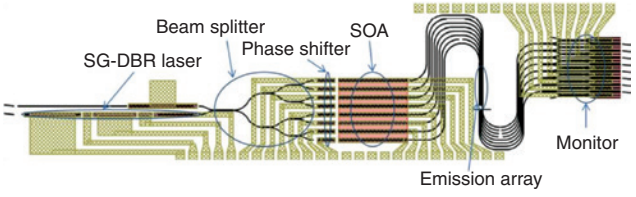

Figure 13: PIC design layout for a fully integrated indium phosphide based OPA, including tunable laser source, phase tuners, optical amplifiers (SOAs), grating emitters, and on-chip phase calibration [38].

can find these along the same lines as the ones mentioned for the tunable-emitter-based OPAs and as discussed in the introduction of this paper. An interesting idea is to use such OPAs in a retroreflective configuration, which would align the OPA automatically to an external transceiver or source-detector combination [41]. This allows, for example, a PIC to receive and transmit data efficiently, without the need for an on-chip source. This makes such an approach very interesting for silicon photonic PICs, as these lack integrated optical sources.

6 Technology outlook and opportunities for future developments and applications

The silicon photonics OPAs discussed have all been realized in mature foundry platforms or in technologies that are very similar and seemingly compatible. Several institutes offer such access at the time of writing, for example, through the Europractice platform [42], and the process reported in Ref. [21] is a commercial IBM process. Similarly,

the indium phosphide OPAs, although an academic proof-of-principle, can likely be fabricated in more mature foundry technologies, such as those offered through the JePPIX platform [43]. This means that such OPAs can in principle be made in a reproducible, high-yield and large-volume process, which should enable the transfer of this technology to industry.

The question remains then whether these PIC-based OPAs can achieve the requirements for real-world applications. PIC technology was and is predominantly used in communications technology, where moderate optical output power levels of 1–20 mW are typical. However, laser diodes are widely used in commercial applications, for example, in high-end Lidar technology for autonomous cars [44]. Obviously, the required laser beam power levels depend on the exact application, e.g. the link length in free-space optical communications and the range of a Lidar system, but some numbers include 0.5-W laser power for coherent Doppler Lidar systems for wind monitoring [45], 80–200 mW for long range free-space optical links of 45–150 km, respectively [46, 47], and multiple watts to tens of watts for countermeasure applications [48].

Although these latter power levels are above the typical PIC based laser diode power levels of up to a few tens of milliwatts maximum [6, 8], PICs offer the advantage of parallelism and the OPA architecture is by definition a power combiner. As argued in Refs. [37, 38], arrays of integrated optical amplifiers can be used to boost the power in single channels to tens of milliwatts, which can then be combined by the emitters into a single beam. The optical damage threshold of, e.g. silicon is about 1–4 GW/cm^2 [49]. The power in a waveguide is typically limited by the nonlinear absorption due to free carriers generated by two-photon absorption in indium phosphide [50] and silicon [51, 52], i.e. not by the two-photon absorption itself. Based on these numbers, it can be expected that the waveguides should be able to handle hundreds of milliwatts optical power without significant losses, i.e. below ~1 dB. So tens of parallel amplifiers or injection-locked lasers can feasibly scale the power out of the OPA into the >1-W regime. Heat dissipation in the area of the PIC where the emitters are located should be considered, though, as grating couplers have finite efficiency and typically around 2-dB loss, which means hundreds of milliwatts are dissipated into a small volume.

Overall device power efficiency is a major performance parameter. For PIC-based OPAs, the contributions are the laser source power consumption, the tuning energy, and the losses in the passive elements, such as the grating couplers, as discussed above. Laser diode efficiency for power levels over ~20 mW and operating in the 1.3 μm–1.6 μm range could typically be around 30% [53]. The energy consumption of the phase tuning elements depends on the physical mechanism, with typical numbers for π-radians switching in the range of 10 nJ–1 μJ for thermo-optic effects, 10 pJ for carrier effects, and 100 fJ for field effects, e.g. the Pockels effect, as per the overview presented in Ref. [54]. For a tuning speed of 100 MHz, this leads to an overall energy consumption of around 10 μW per emitter for field effects and around 1 mW per emitter for carrier effects. For indium phosphide and hybrid silicon OPAs, operating at high output powers of hundreds of milliwatts or more, the energy consumption of the tuning is not necessarily significant. However, for silicon-based OPAs based on a 2D emitter approach, the power consumption would likely be dominated by the tuning power. On top of this, using off-chip lasers leads to an additional hit in efficiency due to the laser coupling efficiency of typically around -2 dB [53]. The length of the phase tuners in silicon and indium phosphide technology is typically in the hundreds of micrometers to millimeters range, which sets a lower limit on the footprint of the PIC. Thermal phase tuners can be more compact but at the cost of lower tuning speed and higher energy consumption [19]. Moreover, if electronics are not integrated monolithically, as was done in Ref. [21], bondpads for all tuning elements need to be added, limiting the footprint further.

Another aspect that real-world implementations have to face is calibration of the PICs. Even when active cooling is used, aging effects, process non-uniformities and finite process tolerances, environmental impact, especially when used as handheld or UAV-mounted devices, can all influence the phase of the emitters in the OPA. This would reduce the efficiency of the beam generation. An OPA can be calibrated offline, by running optimization algorithms on the phase and/or amplitude tuners, using the feedback of an external photodiode, placed at a distance, for example. However, PIC technology has the advantage that such calibration optics can be integrated on the same chip for real-time monitoring of the calibration and for online calibration. Such architectures have been realized in both the hybrid silicon and indium phosphide realizations. In Ref. [38] and as shown in Figure 13, part of the light is transmitted by the emitter gratings and the light of pairs of neighboring channels is combined and monitored using an array of photodiodes. The interference allows for calculating the relative phase between two neighboring channels and, by monitoring the full array, the phase of all channels. Another approach was used in Ref. [37] and shown in Figure 12. An on-chip graded-index lens,

based on a photonic crystal structure, was used to focus a small part of the light after the grating emitters onto an array of photodiodes. The lens converts the near field to a "far-field" pattern on chip, thereby mimicking the emitted field, i.e. the beam and its angle, far away from the PIC [3]. This architecture gives immediate access to the far-field information on the PIC and, hence, allows for on-chip calibration.

As is clear from the above, realizing an OPA with emitter spacing below half the optical output wavelength remains a challenge. Side lobes lead to noise in Lidar systems, to less secure free-space optical links with the risk of eavesdropping, and overall to a decreased optical efficiency. For practical purposes, a field of view of 90°, i.e. ±45°, is suggested [2]. This would lead to a requirement for the emitter spacing of 0.7·λ. This spacing of ~1 μm is still not feasible with the abovementioned technologies. Nevertheless, practical applications do require 30-dB side-lobe suppression, as suggested in Ref. [55]. One approach is to space the emitters non-uniformly to suppress the side lobes, as was already mentioned [14]. This does not increase the power in the main beam, however, and merely smears out the side lobes over a wider range of angles, leading to an increased background. Another approach is to block the side lobes by using an aperture close to and placed at the output of the PIC. Although this limits the steering angle, a lens or curved mirror can be used to magnify the output angle. The drawback is that the beam angle is magnified, too. The technologies and PIC implementations discussed in this review were not able to meet these requirements for field of view and side-lobe suppression yet.

Novel technologies should be considered to avoid the issue of side lobes altogether. Emitters with a severely decreased footprint will then be required, typically called plasmonic antennas or nanoantennas. One example includes a matrix of coupled patch-dipole nanoantennas, as shown in Figure 14, which was used to impose an arbitrary phase profile on the reflection of an incoming beam [56]. In other works, V-shaped antennas [57] and Yagi-Uda nanoantennas [58] were used to achieve the same. Such realizations, although having a close emitter spacing, are passive and lack tuning options. The phase pattern is determined by design and lithography only, so no beam steering can be achieved. Simulations on vanadium dioxide slot nanoantennas show how beam steering can in theory be achieved in such systems. In a 10-element array, the reflection and steering of an incoming beam was simulated by applying a linear temperature gradient over the array. Beam steering of ±22° was shown with a gradient of <10°C [59]. However, individual tuning of the emitters cannot be achieved and the light source in all of these implementations is off-chip.

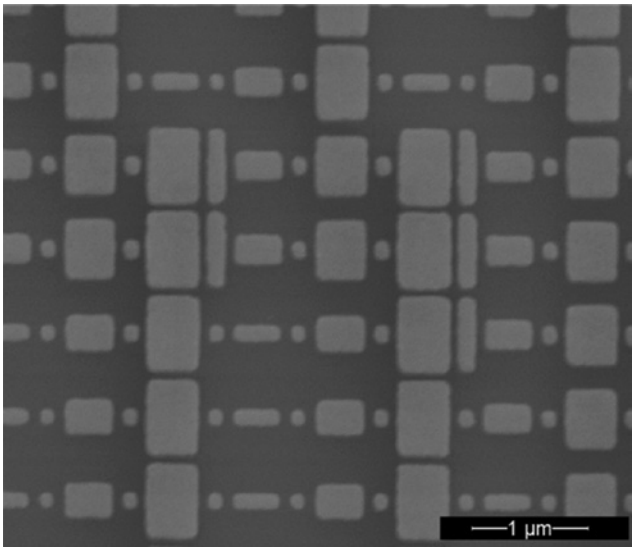

Figure 14: Image of an array of coupled patch-dipole nanoantennas. Reprinted (adapted) with permission from Ref. [56]. Copyright 2014 American Chemical Society.

A promising approach to integrate nanoantennas on a PIC in a mature process was reported in Ref. [60] and shown in Figure 15. This work demonstrates 1×8 phased arrays, having emitter spacings of 6 μm and 9 μm. The emitters are realized by metallic nanoantennas that are evanescently coupled to an underlying silicon waveguide, which guides and distributes the light. Beam steering of 8° was shown, using thermo-optic silicon phase tuners that can tune by 2π radians the individual nanoantennas, as can be seen in Figure 15. Although compact, these phase tuners limit the antenna spacing and lead to side lobes at 14° and 9° for the 6 μm and 9 μm spaced arrays, respectively. This work shows the potential of combining nanoantennas with silicon photonics in terms of tunability and PIC integration density and complexity. But it also shows the issues that remain when active tuning of all emitters is required, namely, the relatively large footprint that is required by the individual emitters when phase control has to be integrated.

To put the PIC-based approach into perspective, this outlook section will be wrapped up with a short overview of alternative approaches, limiting the discussion to technologies that can achieve similar metrics in terms of tuning speed, compactness, and power scaling. A vertical-cavity surface emitting laser (VCSEL) array seems like a natural choice for an OPA. However, such VCSELs are typically not phase locked. In Ref. [61], an approach was outlined how such VCSEL arrays can be made coherent

by injection locking them with a single master laser. Only 1 μW per VCSEL was required to achieve locking. By tuning the VCSEL injection current, a small phase shift can be incurred. To achieve a 1.6π tunable phase shift, two VCSEL arrays were stacked, as shown in Figure 16. These VCSEL arrays contain 64 VCSELs each and are spaced non-uniformly to suppress side lobes. Experimentally 2.2°×1.2° beam steering was achieved in this first realization. This approach has a high potential for power scaling, as the VCSELs can be very efficient and emit directly to free-space, whereas only limited optical power from the master laser is required.

Another alternative approach is the use of MEMS. Although typically slow, with tuning speeds in the millisecond range, so-called high-contrast sub-wavelength gratings (HCGs) have resonant frequencies of 0.32 MHz and can operate in the microsecond range [62]. Figure 17 shows the realization of an 8×8 HCG array, which has to be illuminated with an incident beam. Beam shaping and steering of 1.3°×1.3° was achieved. In Ref. [63], this approach was scaled up to a 32×32 array. For calibration purposes, which is required for real-world applications, as discussed above, an approach using an *in situ* interferometer was proposed and realized in Ref. [64]. This allows for real-time dynamic measurement and control of the phase of MEMS mirrors with an accuracy better than π/100.

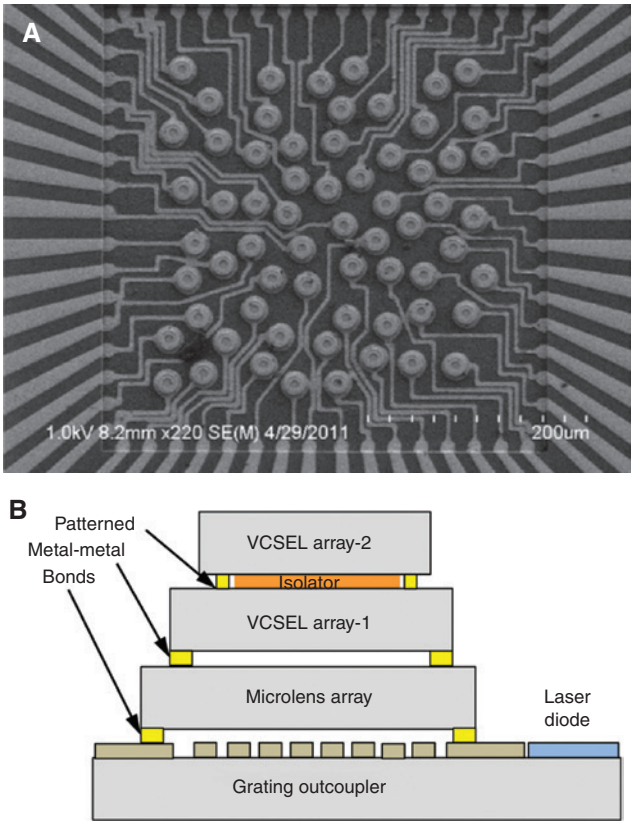

Figure 16: (A) Scanning electron microscopy image of a 64-element non-uniformly spaced VCSEL array, including metal interconnect lines. (B) Schematic of a vertically integrated OPA, including two layers of optically coupled VCSEL arrays. The VCSELs are injection locked to a single, vertically coupled, master laser that is focused on the VCSELs by a microlens array. Reprinted by permission of The Optical Society [61].

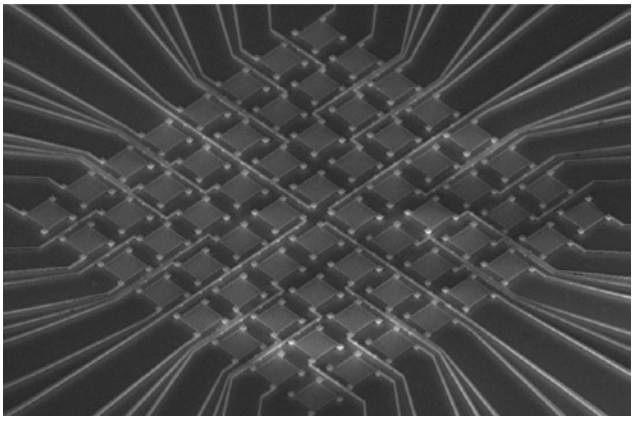

Figure 17: Scanning electron microscopy image of a fabricated 8×8 MEMS HCG array. Reprinted by permission of The Optical Society [62].

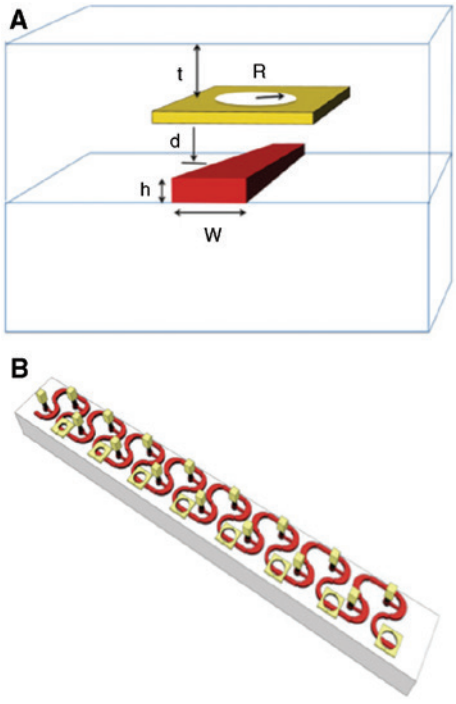

Figure 15: (A) Schematic of the circular aperture antenna (yellow) evanescently coupled to the waveguide (red). (B) A 1×8 linear antenna array schematic with integrated thermo-optic phase shifters. Reprinted by permission of The Optical Society [60].

7 Conclusion

In this paper, I have reviewed the state of the art in PIC-based optical beam shaping and steering chips. PIC technology is maturing fast, showing an exponential growth of integration density and with an on-chip component count exceeding thousands of components per PIC. The current academic proof-of-principle demonstrators show the feasibility for narrow laser beam shaping and steering, although exclusively still in a laboratory environment. Some successful initial applications have been reported, such as projection and depth metrology. Also, on-chip calibration optics has been implemented, which is essential for real-world applications.

Open issues that remain include the power scaling for high-power applications, including Lidar. PIC technology allows in principle for multi-watt output beams, using the parallelism of the channels, but this still needs to be successfully shown. The integration with electronics has been shown on a commercial RF-electronics process, but foundry platforms optimized for photonics, such as the silicon and indium phosphide platforms discussed, will require co-packaging with an electronic integrated circuit. For frame-rate Lidar imaging, such a circuit will need to provide rather high switching powers at switching speeds in the megahertz range. Another packaging consideration is that silicon photonics PICs will require off-chip lasers, unlike indium phosphide and hybrid silicon PICs. This limits output laser power scaling for silicon photonic PICs.

The PIC-based OPAs have been discussed in the context of emerging applications for compact Lidar and free-space optical applications. In terms of optical specifications, PIC technology is compatible with these applications, e.g. with respect to optical output powers and optical wavelengths, which are in the eye-safe range. In terms of SWaP and scanning speed parameters, PIC technology offers the biggest advantage over existing technologies, e.g. enabling portable or drone-mountable systems, and high-speed scanning, beyond the range of current mechanical scanning.

The question remains whether the technology discussed in this work will soon move out of the laboratory into the field for real-world applications. PIC-based technology has often been cost-prohibitive for applications outside telecom and datacom. However, with a maturing technology, which can now be accessed through established foundries, this bottleneck is opening up, and there is a clear path out of the laboratory. This leads to the main conclusion that PIC-based optical beam shaping and steering is a very promising approach for real-world application of, e.g. Lidar and free-space optical communication technologies in the near future where ubiquitous autonomous vehicles, wearables, and sensor systems will dominate our daily life and infrastructure.

Acknowledgments: The author wishes to thank Jonathan Doylend, Leif Johansson, Jared Hulme, Larry Coldren, and John Bowers for useful discussions and insights and collaboration on this topic over many years while he was working at UC Santa Barbara.

References

[1] McManamon PF, Dorschner TA, Corkum DL, Friedman LJ, Hobbs DS, Holz M, Liberman S, Nguyen HQ, Resler DP, Sharp RC, Watson EA. Optical phased array technology. Proc IEEE 1996;84:268–98.

[2] McManamon PF, Bos PJ, Escuti MJ, Heikenfeld J, Serati S, Xie H, Watson EA. A review of phased array steering for narrow-band electrooptical systems. Proc IEEE 2009;97:1078–96.

[3] Goodman JW. Introduction to Fourier optics. Introduction to Fourier optics, 2nd ed. New York, NY: McGraw-Hill, 1996.

[4] Dumon P, Bogaerts W, Baets R, Fedeli JM, Fulbert L. Towards foundry approach for silicon photonics: silicon photonics platform ePIXfab. Electron Lett 2009;45:581–2.

[5] Hochberg M, Baehr-Jones T. Towards fabless silicon photonics. Nat Photon 2010;4:492–4.

[6] Smit M, Leijtens X, Ambrosius H, Bente E, van der Tol J, Smalbrugge B, de Vries T, Geluk E-J, Bolk J, van Veldhoven R, Augustin L, Thijs P, D'Agostino D, Rabbani H, Lawniczuk K, Stopinski S, Tahvili S, Corradi A, Kleijn E, Dzibrou D, Felicetti M, Bitincka E, Moskalenko V, Zhao J, Santos R, Gilardi G, Yao W, Williams K, Stabile P, Kuindersma P, Pello J, Bhat S, Jiao Y, Heiss D, Roelkens G, Wale M, Firth P, Soares F, Grote N, Schell M, Debregeas H, Achouche M, J-L Gentner, Bakker A, Korthorst T, Gallagher D, Dabbs A, Melloni A, Morichetti F, Melati D, Wonfor A, Penty R, Broeke R, Musk B, Robbins D. An introduction to InP-based generic integration technology. Semicond Sci Technol 2014;29:083001.

[7] A Leinse, RG Heideman, M Hoekman, Schreuder F, Falke F, Roeloffzen CGH, Zhuang L, Burla M, Marpaung D, Geuzebroek DH, Dekker R, EKlein J, van Dijk PWL, Oldenbeuving RM. TriPleX waveguide platform: low-loss technology over a wide wavelength range. In SPIE Microtechnologies 2013 May 22 (pp. 87670E-87670E). Bellingham, Washington, USA: International Society for Optics and Photonics.

[8] Heck MJ, Bauters JF, Davenport ML, Doylend JK, Jain S, Kurczveil G, Srinivasan S, Tang Y, Bowers JE. Hybrid silicon photonic integrated circuit technology. IEEE J Sel Topics Quantum Electron 2013;19:6100117.

[9] Sacher WD, Huang Y, Lo GQ, Poon JK. Multilayer Silicon Nitride-on-Silicon Integrated Photonic Platforms and Devices. J Lightwave Technol 2015;33:901–10.

[10] Bauters JF, Davenport ML, Heck MJ, Doylend JK, Chen A, Fang AW, Bowers JE. Silicon on ultra-low-loss waveguide photonic integration platform. Opt Express 2013;21:544–55.

[11] Piels M, Bauters JF, Davenport ML, Heck MJ, Bowers JE. Low-loss silicon nitride AWG demultiplexer heterogeneously integrated with hybrid III–V/silicon photodetectors. J Lightwave Technol 2014;32:817–23.
[12] Heck MJ, Bauters JF, Davenport ML, Spencer DT, Bowers JE. Ultra-low loss waveguide platform and its integration with silicon photonics. Laser Photon Rev 2014;8:667–86.
[13] Flamand G, De Mesel K, Moerman I, Dhoedt B, Hunziker W, Kalmar A, Baets R, Van Daele P, Leeb W. InP-based PIC for an optical phased-array antenna at 1.06 m. IEEE Photonics Technol Lett 2000;12:876–8.
[14] Kwong D, Hosseini A, Zhang Y, Chen RT. 1×12 Unequally spaced waveguide array for actively tuned optical phased array on a silicon nanomembrane. Appl Phys Lett 2011;99:051104.
[15] Hosseini A, Kwong D, Zhang Y, Chandorkar SA, Crnogorac F, Carlson A, Fallah B, Bank S, Tutuc E, Rogers J, Pease RFW, Chen RT. On the fabrication of three-dimensional silicon-on-insulator based optical phased array for agile and large angle laser beam steering systems. J Vac Sci Technol B 2010;28:C6O1–7.
[16] Thomson RR, Birks TA, Leon-Saval SG, Kar AK, Bland-Hawthorn J. Ultrafast laser inscription of an integrated photonic lantern. Opt Express 2011;19:5698–705.
[17] Mekis A, Gloeckner S, Masini G, Narasimha A, Pinguet T, Sahni S, De Dobbelaere P. A grating-coupler-enabled CMOS photonics platform. IEEE J Sel Topics Quantum Electron 2011;17:597–608.
[18] Vermeulen D, Selvaraja S, Verheyen P, Lepage G, Bogaerts W, Absil P, Van Thourhout D, Roelkens G. High-efficiency fiber-to-chip grating couplers realized using an advanced CMOS-compatible silicon-on-insulator platform. Opt Express 2010;18:18278–83.
[19] Sun J, Timurdogan E, Yaacobi A, Hosseini ES, Watts MR. Large-scale nanophotonic phased array. Nature 2013;493:195–9.
[20] Sun J, Yaacobi A, Cole DB, Leake G, Coolbaugh D, Watts MR. Two-dimensional apodized silicon photonic phased arrays. Opt Lett 2014;39:367–70.
[21] Abediasl H, Hashemi H. Monolithic optical phased-array transceiver in a standard SOI CMOS process. Opt Express 2015;23:6509–19.
[22] Aflatouni F, Abiri B, Rekhi A, Hajimiri A. Nanophotonic projection system. Opt Express 2015;23:21012–22.
[23] Aflatouni F, Abiri B, Rekhi A, Hajimiri A. Nanophotonic coherent imager. Opt Express 2015;23:5117–25.
[24] Gerchberg RW, Saxton WO. Phase retrieval by iterated projections. Optik 1972;35:237.
[25] Fienup JR. Phase retrieval algorithms: a comparison. Appl Opt 1982;21:2758–69.
[26] Coldren LA, Fish GA, Akulova Y, Barton JS, Johansson L, Coldren CW. Tunable semiconductor lasers: a tutorial. J Lightwave Technol 2004;22:193.
[27] Fujioka N, Chu T, Ishizaka M. Compact and low power consumption hybrid integrated wavelength tunable laser module using silicon waveguide resonators. J Lightwave Technol 2010;28:3115–20.
[28] Hulme JC, Doylend JK, Bowers JE. Widely tunable Vernier ring laser on hybrid silicon. Opt Express 2013;21:19718–22.
[29] Keyvaninia S, Roelkens G, Van Thourhout D, Jany C, Lamponi M, Le Liepvre A, Lelarge F, Make D, Duan G-H, Bordel D, Fedeli J-M. Demonstration of a heterogeneously integrated III-V/SOI single wavelength tunable laser. Opt Express 2013;21:3784–92.
[30] Van Acoleyen K, Bogaerts W, Jágerská J, Le Thomas N, Houdré R, Baets R. Off-chip beam steering with a one-dimensional optical phased array on silicon-on-insulator. Opt Lett 2009;34:1477–9.
[31] Doylend JK, Heck MJ, Bovington JT, Peters JD, Coldren LA, Bowers JE. Two-dimensional free-space beam steering with an optical phased array on silicon-on-insulator. Opt Express 2011;19:21595–604.
[32] Van Acoleyen K, Rogier H, Baets R. Two-dimensional optical phased array antenna on silicon-on-insulator. Opt Express 2010;18:13655–60.
[33] Van Acoleyen K, Bogaerts W, Baets R. Two-dimensional dispersive off-chip beam scanner fabricated on silicon-on-insulator. IEEE Photonics Technol Lett 2011;23:1270–2.
[34] Kwong D, Hosseini A, Covey J, Zhang Y, Xu X, Subbaraman H, Chen RT. On-chip silicon optical phased array for two-dimensional beam steering. Opt Lett 2014;39:941–4.
[35] Roelkens G, Van Thourhout D, Baets R. High efficiency silicon-on-insulator grating coupler based on a poly-silicon overlay. Opt Express 2006;14:11622–30.
[36] Doylend JK, Heck MJR, Bovington JT, Peters JD, Davenport ML, Coldren LA, Bowers JE. Hybrid III/V silicon photonic source with integrated 1D free-space beam steering. Opt Lett 2012;37:4257–9.
[37] Hulme JC, Doylend JK, Heck MJR, Peters JD, Davenport ML, Bovington JT, Coldren LA, Bowers JE. Fully integrated hybrid silicon two dimensional beam scanner. Opt Express 2015;23:5861–74.
[38] Guo W, Binetti PRA, Althouse C, Masanovic ML, Ambrosius HPMM, Johansson LA, Coldren LA. Two-dimensional optical beam steering with InP-based photonic integrated circuits. IEEE J Sel Topics Quantum Electron 2013;19:6100212.
[39] He L, Liu Y, Galland C, Lim AE, Lo GQ, Baehr-Jones T, Hochberg M. A high-efficiency nonuniform grating coupler realized with 248-nm optical lithography. IEEE Photonics Technol Lett 2013;25:1358–61.
[40] Heck MJ. Grating coupler enabled optical isolators and circulators for photonic integrated circuits. IEEE J Sel Topics Quantum Electron 2015;21:1–9.
[41] Van Acoleyen K, O'Brien DC, Payne F, Bogaerts W, Baets R. Optical retroreflective marker fabricated on silicon-on-insulator. IEEE Photonics J 2011;3:789–98.
[42] http://www.europractice-ic.com/SiPhotonics_general.php, *viewed d.d. 11-19-2015*.
[43] www.jeppix.eu/, *viewed d.d. 11-19-2015*.
[44] Schwarz B. LIDAR: Mapping the world in 3D. Nat Photon 2010;4:429–30.
[45] Rodrigo PJ, Pedersen C. Field performance of an all-semiconductor laser coherent Doppler Lidar. Opt Lett 2012;37:2277–9.
[46] Biswas A, Ceniceros JM, Novak MJ, Jeganathan M, Portillo A, Erickson DM, De Pew J, Sanii Bx, Lesh JR. 45-km horizontal-path optical link experiment. In Optoelectronics' 99-Integrated Optoelectronic Devices 1999 Apr 26 (pp. 43–53). Bellingham, Washington, USA: International Society for Optics and Photonics.
[47] Neo SS. Free space optics communication for mobile military platforms. Naval Postgraduate School Monterey, CA, 2003.
[48] Wagner J, Schulz N, Rösener B, Rattunde M, Yang Q, Fuchs F, Manz C, Bronner W, Mann C, Köhler K, Raab M, Romasev E, Tholl HD. Infrared semiconductor lasers for DIRCM

applications. In SPIE Europe Security and Defence 2008 Oct 2 (pp. 71150A–71150A). Bellingham, Washington, USA: International Society for Optics and Photonics.
[49] Jalali B, Raghunathan V, Shori R, Fathpour S, Dimitropoulos D, Stafsudd O. Prospects for silicon mid-IR Raman lasers. IEEE J Sel Topics Quantum Electron 2006;12:1618–27.
[50] Van Thourhout D, Doerr CR, Joyner CH, Pleumeekers JL. Observation of WDM crosstalk in passive semiconductor waveguides. IEEE Photonics Technol Lett 2001;13:457–9.
[51] Liang TK, Tsang HK. Role of free carriers from two-photon absorption in Raman amplification in silicon-on-insulator waveguides. Appl Physics Lett 2004;84:2745–7.
[52] Claps R, Raghunathan V, Dimitropoulos D, Jalali B. Influence of nonlinear absorption on Raman amplification in silicon waveguides. Opt Express 2004;12:2774–80.
[53] Heck MJ, Bowers JE. Energy efficient and energy proportional optical interconnects for multi-core processors: driving the need for on-chip sources. IEEE J Sel Topics Quantum Electron 2014;20:332–43.
[54] Liu K, Ye CR, Khan S, Sorger VJ. Review and perspective on ultrafast wavelength-size electro-optic modulators. Laser Photon Rev 2015;9:172–94.
[55] DARPA Broad Agency Announcement DARPA-BAA-09-66. Short-range Wide-field-of-view Extremely-agile Electronically-steered Photonic EmitteR (SWEEPER). Microsystems Technology Office. June 24, 2009 (As Amended on 9 July 2009).
[56] Yifat Y, Eitan M, Iluz Z, Hanein Y, Boag A, Scheuer J. Highly efficient and broadband wide-angle holography using patch-dipole nanoantenna reflectarrays. Nano Lett 2014;14:2485–90.
[57] Aieta F, Genevet P, Yu N, Kats MA, Gaburro Z, Capasso F. Out-of-plane reflection and refraction of light by anisotropic optical antenna metasurfaces with phase discontinuities. Nano Lett 2012;12:1702–6.
[58] Dregely D, Taubert R, Dorfmüller J, Vogelgesang R, Kern K, Giessen H. 3D optical Yagi-Uda nanoantenna array. Nat Commun 2011;2:267.
[59] Kaplan G, Aydin K, Scheuer J. Dynamically controlled plasmonic nano-antenna phased array utilizing vanadium dioxide. Opt Mater Express 2015;5:2513–24.
[60] DeRose CT, Kekatpure RD, Trotter DC, Starbuck A, Wendt JR, Yaacobi A, Watts MR, Chettiar U, Engheta N, Davids PS. Electronically controlled optical beam-steering by an active phased array of metallic nanoantennas. Opt Express 2013;21:5198–208.
[61] Sayyah K, Efimov O, Patterson P, Schaffner J, White C, Seurin JF, Xu G, Miglo A. Two-dimensional pseudo-random optical phased array based on tandem optical injection locking of vertical cavity surface emitting lasers. Opt Express 2015;23:19405–16.
[62] Yoo BW, Megens M, Chan T, Sun T, Yang W, Chang-Hasnain CJ, Horsley DA, Wu MC. Optical phased array using high contrast gratings for two dimensional beamforming and beamsteering. Opt Express 2013;21:12238–48.
[63] Yoo BW, Megens M, Chan TK, Sun T, Yang W, Horsley DA, Chang-Hasnain CJ, Wu MC. 32×32 Optical phased array with ultra-lightweight high-contrast-grating mirrors. In Solid-State Sensors, Actuators and Microsystems (TRANSDUCERS & EUROSENSORS XXVII), 2013 Transducers & Eurosensors XXVII: The 17th International Conference on 2013 Jun 16 (pp. 2505–2508). Piscataway, NJ, USA: IEEE.
[64] Chan TK, Megens M, Yoo BW, Wyras J, Chang-Hasnain CJ, Wu MC, Horsley DA. Optical beamsteering using an 8×8 MEMS phased array with closed-loop interferometric phase control. Opt Express 2013;21:2807–15.